doi: 10.5028/jatm.v5i3.223

Optimal Design of a High-Altitude Solar-Powered Unmanned Airplane

Bento Silva de Mattos[1], Ney Rafael Secco[1], Eduardo Francisco Salles[1]

ABSTRACT: This paper describes a multi-disciplinary design and optimization framework tailored for the conceptual development of high-altitude solar-powered unmanned aerial vehicles. The aircraft baseline configuration that the framework is able to handle is very similar to that of Zephyr, which is developed by the UK based company QinetiQ. The disciplines of aerodynamics, structures, stability, weight, and systems were considered and integrated into a modeFrontier® workflow, capable of providing a relatively simple sizing, but highly realistic airplane.

KEYWORDS: Airplane design, Solar energy, Multi-disciplinary design and optimization, Airplane stability and control.

INTRODUCTION

The present work is concerned with the optimal design of unmanned high-altitude long-endurance (HALE) solar-powered airplanes. In order to accomplish this, a multi-disciplinary design framework was elaborated employing the modeFrontier® (ESTECO, 2011) commercial optimization package. A brief technical retrospective of the development on solar-driven aircraft is provided in this section as well as the reasoning to address the utilization of such kind of airplane.

The first flight of a solar-powered aircraft took place on November 4th, 1974, when the remotely controlled Sunrise I, designed by Robert J. Boucher of AstroFlight, Inc., flew after a catapult launch (Noth, 2008). The flight lasted 20 minutes at an altitude of around 100 m (Noth, 2008).

AeroVironment, Inc. was founded in 1971 by the ultra-light airplane innovator Paul MacCready. Following the AstroFlight's airplane debut, AeroVironment undertook a more ambitious project to design a human-piloted, solar-powered aircraft. The firm initially based its design on the human-powered Gossamer Albatross II and scaled it down to three-quarters of its previous size for solar-powered flights. This was easier to accomplish because, in early 1980, the Gossamer Albatross aircraft had participated in a flight research program at NASA Dryden Research Center. Some of the Albatross flights were performed employing a small electric motor. The scaled-down aircraft was designated Gossamer Penguin (Fig. 1). It had a 71-ft wingspan compared to the 21.64-m (96-ft) span of the Gossamer Albatross (MacCready et al., 1983). Penguin's Empty Weight was just 31 kg, it had a low-power requirement and, therefore, it was an excellent test bed for testing of solar power systems (Noth, 2008).

1.Instituto Tecnológico de Aeronáutica – São José dos Campos/SP – Brazil

Author for correspondence: Bento Silva de Mattos | Instituto Tecnológico de Aeronáutica | Praça Marechal Eduardo Gomes, 50 – Vila das Acácias | CEP 12.228-900 São José dos Campos/SP – Brazil | Email: baviator@gmail.com

Received: 17/12/12 | **Accepted:** 10/04/13

Figure 1. The first piloted solar plane, the Gossamer Penguin.

AstroFlight, Inc., of Venice, California, provided the power plant for the Gossamer Penguin, an Astro Cobalt 40 electric motor. This engine was designed to run at between 10,000 and 15,000 rpm, but the 11-ft diameter propeller of Penguin rotates between 120 and 130 rpm. The speed reduction was achieved with a three-stage gearbox with two timing pulley stages providing a reduction ratio of 5/1 each and a final chain reduction stage delivering a 5.12/1 ratio. Robert Boucher, designer of the Sunrise II, worked as a key consultant for both aircraft and for the Solar Challenger. The power source for the initial flights of the Gossamer Penguin consisted of 25 nickel-cadmium batteries and panels of 3,640 solar cells delivering 541W. The battery-powered flights took place at Shafter Airport near Bakersfield, California. Paul MacCready's son, Marshall, was the test pilot. He was 13 years old and weighed approximately 80 lb (36 kg) at that time. The main targets of the test flights were the determination of required power to fly the airplane, the optimization of the airframe/propulsion system, and pilot training. Flights took place on April 7th, 1980, and a short solar-powered one on May 18th. However, the official project pilot was Janice Brown, a Bakersfield school teacher who weighed in at slightly less than 45 kg and was a charter pilot with commercial, instrument, and glider ratings. She checked out in the plane at Shafter and made about 40 solar-powered flights. Wind direction, turbulence, convection, temperature and radiation at Shafter in mid-summer proved to be less than ideal for Gossamer Penguin because of crosswinds at takeoff and decreased solar power output due to higher ambient temperatures. Consequently, the project moved to Dryden in late July, although conditions there also were not ideal. Nevertheless, Janice finished the testing, and on August 7th, 1980, she flew a public demonstration at Dryden in which she was able to cover 3.14 km in 14 minutes and 21 seconds. This was significant as the first sustained flight of an aircraft relying solely on direct solar power rather than batteries. It provided the designers with practical experience for developing a more efficient solar-powered aircraft, taking into account that the Gossamer Penguin was fragile and had limited controllability. The Penguin flew preferably in the morning, when usually wind is minimal and consequently the turbulence level is still low. On the other hand, at this part of the day, the angle of the sun was low, requiring a tilting solar panel to capture properly the solar radiation (Noth, 2008).

From the lessons learned with Gossamer Penguin, AeroVironment engineering staff designed Solar Challenger, a piloted, solar-powered aircraft that was capable of high-altitude and long-endurance flights (Noth, 2008).

The last big step in aircraft powered by solar energy is the first flight of twin-engine Solar Impulse airplane on December 3rd, 2009 (Solar Impulse, 2013). Solar Impulse is a long-range solar powered plane project currently being undertaken at the École Polytechnique Fédérale in Lausanne, Switzerland. The project is promoted by Bertrand Piccard, who piloted the first balloon that was able to circumnavigate the world nonstop. This project is expected to repeat that milestone in aviation history by employing a solar-powered airplane. The first aircraft, officially named HB-SIA, is able to accommodate a single pilot, capable of taking off under its own power, and is intended to remain airborne up to 36 hours. Building on the experience of this prototype, a slightly larger follow-on design (HB-SIB) is planned to make circumnavigation of the globe in 20-25 days. On April 7th, 2010, the HB-SIA underwent an extended 87 minutes test flight (Fig. 2). In contrast to earlier tests, the April flight reached an altitude of 1,200 m (3,937 ft). In February 2012, Solar Impulse pilot Andre Borschberg spent more than 60 hours straight at the controls of the Solar Impulse flight simulator (Fig. 3). Granted, he was able to get some sleep, sometimes napping for a whole 20 minutes at a time (Solar Impulse, 2013). At that time, Borschberg was approaching the end of a 72-hour stint in the simulator, running through a series of tests and challenges to prepare for what lies ahead

Figure 2. Solar Impulse flight on April 7th, 2010.

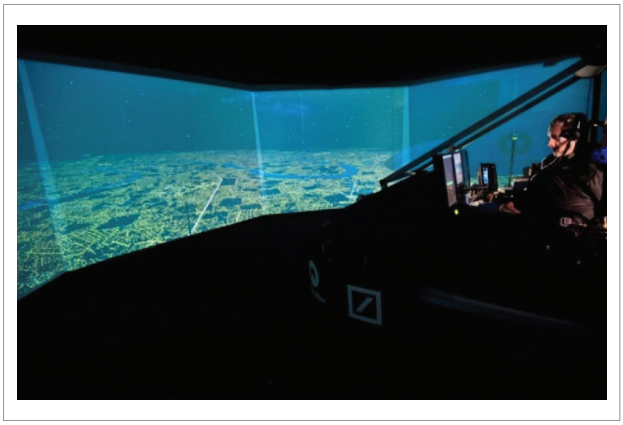

Figure 3. Solar Impulse flight simulator.

simultaneously (Romeo and Frulla, 2004). This means a user community of 8.5 million per unit (although this does not take into account data transmission).

The UAV platform of major interest to the present work is one that is capable to reach stratospheric altitudes and long endurance flights (HALE category) and powered by solar energy. In this context, the Zephyr, developed by the UK based QinetiQ (QinetiQ, 2013), is a configuration that is very similar to that envisaged by the authors. The airplane carries a small payload and has no need for sophisticated assisted takeoff systems or prepared airfields (Fig. 4). The Zephyr is a lightweight airplane

Figure 4. QinetiQ's Zephyr during an assisted take off run (Photo: QinetiQ, 2013).

when he attempts to fly around the world in a solar airplane in 2014 (Solar Impulse, 2013).

In recent years, European countries are taking a more central role in the development of High Altitude/Long Endurance solar-powered unmanned aerial vehicles (UAVs). Several projects are either ongoing or being planned for advanced solar powered vehicles. In the 2000–2003 period, a team from the Politecnico de Torino, in Italy, together with a team from the University of York in the UK, developed a concept for the Heliplat – a Very-Long Endurance Solar Powered Autonomous Aircraft (VESPAA) (Romeo and Frulla, 2004). Heliplat and other VESPAA UAVs could play the role of a "pseudo satellite", with the advantages of being closer to the ground, more flexible and at a cost lesser than an actual satellite. Heliplat-like HALE flying above a major city will be able to cover a circular area of 1,000 km diameter, and process a predicted 425,000 cell phone conversations that uses a combination of a solar array and batteries to stay airborne. The plane weighs just 31 kg and has a wingspan of about 18 m (QinetiQ, 2013). The vehicle can circle over a particular area for extended periods. The military uses the vehicle for reconnaissance and communications platforms. Civilian and scientific programs use it for Earth observation. During the day, Zephyr uses its state-of-the-art solar cells spread across its wings to recharge high-power lithium-sulphur batteries and drive two propellers. At night, the energy stored in the batteries is sufficient to keep Zephyr airborne. The batteries are supplied by Sion. In 2008, the airplane registered a recorded flight, staying airborne for a total of 82 hours and 37 minutes, which is a very impressive number for a solar powered air vehicle (QinetiQ, 2013). The Zephyr went for two straight nights without stopping for recharging and only relying on its solar powered batteries. The airplane is able to climb to altitudes up to 18 km (58,000 ft) (QinetiQ, 2013).

Missions conceived for Zephyr include forest and ocean monitoring, surveillance, and communication relay. Some highlights of Zephyr configuration:

- Zephyr's low-weight structure allows it to travel non-stop over long distances or to remain airborne in a desired station for a considerable long time.
- The unique propeller design provides the aircraft with a higher power-to-weight ratio.
- The aircraft flies day and night powered by solar energy – recharging its batteries along the day.
- No complex launching mechanisms – the aircraft is launched manually by a ground crew of three people.
- Silent flight – neither noise nor pollutant emissions.
- The wing design takes into account thermal air currents to lift the aircraft to higher altitudes.

METHODOLOGY

Before starting with the design of any solar-powered aerial vehicle, it is important to establish how the solar energy will be converted into vehicle motion (propulsion) and how to provide power for the airplane systems. Usually, the wing is an appropriate place to be covered with solar cells, which collect solar radiation and transform it into electrical energy. Batteries, propulsion and systems operate under different conditions and thus a converter package is necessary. An appliance called Maximum Power Point Tracking (MPPT) enables the extraction of maximum power of solar cells and supplies the aircraft systems. During night, there is considerably less energy from solar cells and battery shall fulfill all power needs. Some modern solar cells are able to convert the infrared night radiation into electric power, enabling the batteries continuously to be loaded. This kind of solar cell was not considered in the present work. Figure 5 provides a scheme of the energy management inside the aircraft.

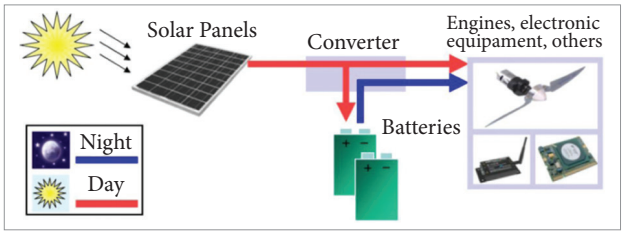

Figure 5. Solar energy conversion system to power engine and other aircraft systems.

SOLAR IRRADIATION MODELS

For a better understanding of the power system, it is necessary to describe the solar radiation model and the systems responsible for its transformation into useful energy.

In order to proceed with the calculation of the solar panel area required on the airplane, it is necessary to estimate the available solar radiation in a given location and date. For this, the relative movement of the Earth around the Sun and of our planet around its axis must be well understood.

The Earth has an elliptical orbit around the Sun, with an average distance of 150 million km. Period of revolution is of 365 days and 4 hours. On January 1st, the nearest distance between our planet and the Sun takes place (perihelion); and on July 1st, the remotest position, the distance is 3.3% farther than that of the closest position (aphelion). Considering that the incident solar radiation is inversely proportional to the square of the distance, the perihelion receives around 7% more radiation than when the Earth is at the aphelion. Another four points also are very important in the astronomy: the autumn and spring equinoxes; and summer and winter solstices (Fig. 6).

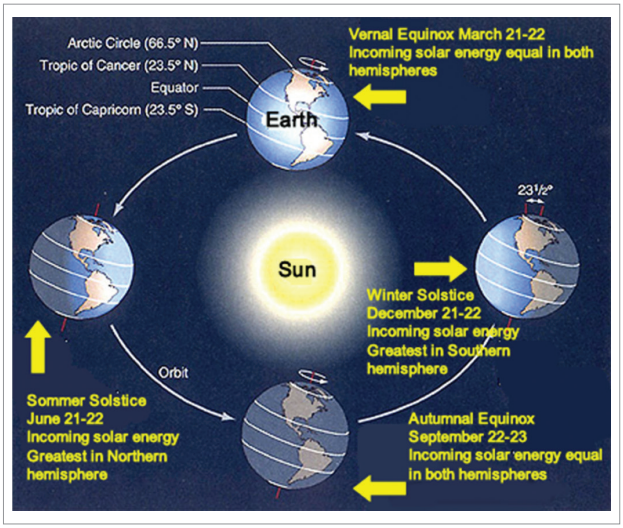

Figure 6. Reference points of Earth's orbit.

The perihelion and the aphelion are the days of most and least intense radiation, respectively. The summer and winter solstices are the days with the longest and shortest time of solar radiation exposure. Being conservative, it is considered that the aircraft should able to fly in any condition and so the point of project is the critical day of the year, in which it receives the least radiation along the day.

The solar irradiance models found in the literature are based on data collected in the Northern hemisphere, mainly in the United States and Europe. For the present work, the model R.SUN was employed (IET, 2013). This sophisticated model was distributed by the Photovoltaic Geographical Information System (PVGIS) of the European Union. PVGIS provides online interactive maps of photovoltaic potentials in Europe and Africa. Figure 7 shows such a map considering the yearly sum of solar electricity generated by 1 kWp system with optimally-inclined modules. R.SUN was developed for the European and Africa environment and it is able to predict the direct and diffuse irradiation and that reflected by the Earth's surface. This last part of the solar irradiation is not taken into account in the present work, since the solar panels are located on the wing upper side of our solar-powered UAV.

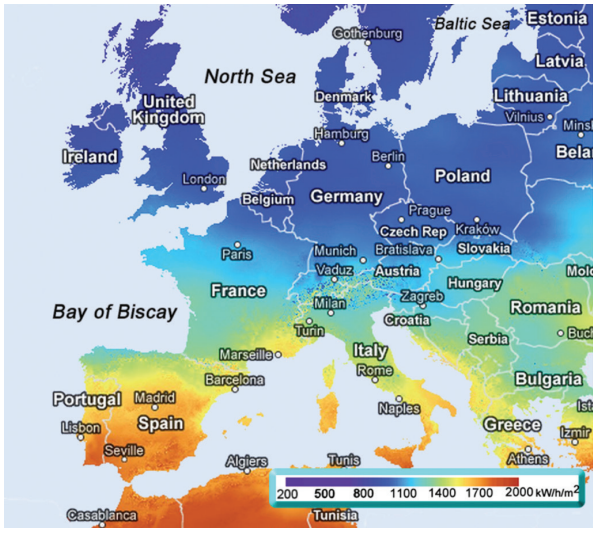

Figure 7. Photovoltaic solar electricity potential in European countries (Source: Photovoltaic Geographical Information System of European Union).

R.SUN is able to estimate the solar irradiation according to latitude, altitude, date and time of the day. In this way, it can be computed the radiation accumulated during an unclouded day. From this estimation, an example of density of energy per area is shown in Fig. 8.

According to the R.SUN model, for an aircraft at 40°N latitude and flying 16 km above sea level, the critical day is December 21st. In this day, the distribution of radiation is shown in Fig. 6. The chosen latitude is the reference for the irradiation model. The power demand should be easily achieved in the inter-tropical region, where Brazil is located, since the incident radiation is larger there.

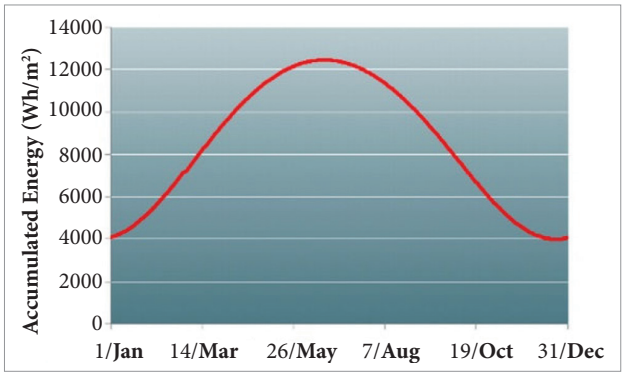

Figure 8. Yearly variation of accumulated daily radiation.

ELECTRICAL LOAD

In the preceding paragraphs, the available power from solar irradiation was outlined. In this section, the concern is with the electrical power demand for the aircraft.

Power required for the payload package can vary. For this reason, an electrical demand of 100 and 200 W was considered. Power required for the control systems actuators is estimated to be 25.5 W. The engine power can be modeled in the following way (Eq. 1; Anderson, 1989):

$$P = \frac{C_D}{C_L^{1.5}} \sqrt{\frac{(mg)^3}{S} \frac{2}{\rho}} \qquad (1)$$

QinetiQ's Zephyr presents an estimated electrical load of 174 W. This figure occurs close to the stall condition, being necessary to adopt a safety margin. There are some power losses in the power plant system that increase the required power to operate the airplane. Such losses are caused by the propeller, the control box, the engine, and the gearbox, which present efficiencies of 87, 95, 95, and 95%, respectively (Noth, 2008; Roskam, 2000). Taking into account such losses, the required weight-to-power ratio tops 100 kg/hp. Thus, the cruise is not the most critical condition to define the required power. Some critical maneuvers must be addressed for such purpose. The airplane must be able to handle gusts and other severe operating conditions. However, in the present work, the used approach was based on similar weight-to-power ratios at cruise

Table 1. Weight to nominal power ratio for some solar-powered airplanes (Noth, 2008).

Airplane	Weight-to-power ratio (kg/hp)
Solar challenger	60.98
Pathfinder	29.53
Pathfinder plus	23.77
Centurion	27.46
Zephyr (estimated)	22.37

of some solar-powered planes (Table 1). The adopted value was slightly higher than that one of Zephyr: 25 kg/hp.

Typical cruise power for electrical driven airplanes is 56% of the engine nominal power. Thus, for the Zephyr airplane, this represents an increase of 140% and the adopted figure for the present work airplane was of 17.9 kg/hp.

ACTUATORS

Actuators are employed in control surfaces like ailerons, rudder, and elevators. The airplane under development is configured with no high-lift devices and presents no landing gear. German company Volz is the actuator supplier for the Zephyr UAV (Volz Servos, 2013). The temperature of operation for usual actuator varies from 30 to 70ºC. However, in the tropopause, the typical temperature is -56.5ºC. For this reason, they developed a special actuator able to withstand temperatures below -70ºC – model DA 13-05-EXP 11859 (Fig. 9).

All actuators of the DA-13-05 Volz family have the same size (37.4x34.9x13.3 mm), operating voltage (4.8 to 5 V), angle (130°), and casing mass (19 g) but they differ by available output torque, device rotating speed and electrical current (power) (Volz Servos, 2013). Zephyr's actuator is the most advanced available on market in its class. However, there is no public data available and therefore we adopted the specification of the DA 13-05-60 device.

SOLAR PANELS AND BATTERIES

The solar panels are extremely important components, considering that they are the unique source of energy, except the charged batteries in the first day of operation. The impact of solar panels on the project is unquestionable. Their development was recorded to be slow and always has been a critical bottleneck for this kind of airplane. For example, Pathfinder and Pathfinder Plus were developed with the same characteristics, at the same time and using the same technology, and by the same team. However, they differ in service ceiling, which is about 30,000 ft for the Plus version thanks to increased efficiency of solar panels.

Several characteristics of state-of-art solar panels were compared, among them the efficiency and weight per area. Flexible panels (Fig. 10) were then selected. Both specific weights are very similar and they can be considered as ultra-light panels. Efficiency is the factor that was taken into account for panel selection as well. In a conservative way, in this study we consider ISA+15 atmosphere conditions, as the efficiency increases with decreasing temperature. As result, the panel

Figure 9. Volz actuator DA 13-05.

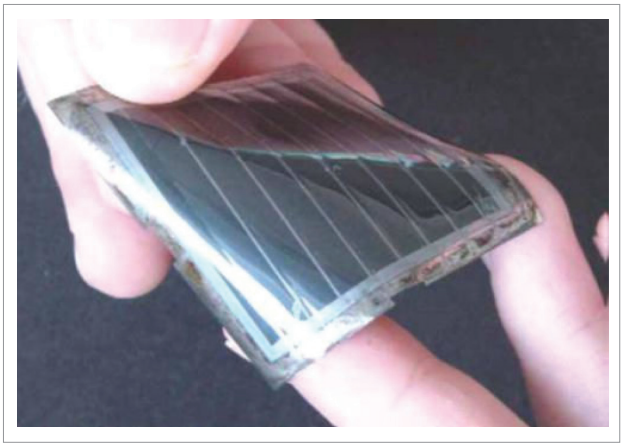

Figure 10. High-flexible and low-weight solar panels.

with Copper indium gallium selenide (CIGS) technology produced by Swiss company Flisom was selected, providing maximum efficiency of 18.8% (Flisom, 2013).

The most used batteries for portable equipment have lithium in their composition. However, a new generation of batteries based on chemical reaction between lithium and sulfur is available, but the concept is experimental stage. The advantages are weight and volume reduction for the same charge capacity. Lithium-sulfur batteries made by Sion Power are very advanced and some versions have specific energy above 265 Wh/kg (Volz Servos, 2013), value that was adopted in the present study.

Sion Power lithium sulfur (Li-S) batteries were fitted into the Zeyphr airplane in 2010. The batteries played a critical role in the QinetiQ Zephyr smashing the world record for the longest duration unmanned flight. As a result of an intensive joint development effort between Sion Power and QinetiQ, the Zephyr flight exceeded 336 hours (14 days) of continuous flight, significantly surpassing the previous official record of 30 hours 24 minutes set by Northrop Grumman's RQ-4A Global Hawk in March 2001 (Sion Power™, 2013). The Zephyr's world record flight was completed on July 23, 2010, at the US Army's Yuma Proving Grounds in Yuma, Arizona (Sion Power™, 2013).

OPTIMIZATION FRAMEWORK

The simulations for the airplane design under consideration were carried out by using the commercial software package modeFrontier® V4.3 (ESTECO, 2011). The optimization framework modeFRONTIER provides a multi-objective optimization and design environment and it easily enables the coupling of CAD/computer aided engineering (CAE) tools, finite element structural analysis and computational fluid dynamics (CFD) software. It is developed by ESTECO SpA and provides an environment for product engineers and designers (ESTECO, 2011). ModeFRONTIER® is a Graphical User Interface (GUI) driven software written in Java that wraps around the CAE tool, performing the optimization by modifying the value assigned to the input variables, and analyzing the outputs as they can be defined as objectives and/or constraints of the design problem.

In the present work, the airplane configuration that was select for study is very similar to that of the monoplane Qinetiq Zephyr, i.e., featuring a rectangular wing with a conventional tail, which is connected to the wing by a boom. The two engines are located at the inner wing.

The design variables of the present optimization framework are given in Table 2. No geometric wing twist was considered. Two electrical power requirements related to two different payloads were simulated: 100 and 200 W.

Table 2. Design variables.

Variable	Description
AR_w	Wing aspect ratio
AR_{HT}	Horizontal stabilizer aspect ratio
AR_{VT}	Vertical stabilizer aspect ratio
S_w	Wing area
CVH	Horizontal tail volume coefficient
CVT	Vertical tail volume coefficient
y_q	Location of the break station of the wing
L_H	Horizontal tail arm
L_V	Vertical tail arm
Φ_w	Outer wing dihedral angle
T_{Config}	Tail configuration (=0: conventional; =1: "T" tail)

It is reasonable to assume that a lighter airplane will be cheaper. Airplane size is proportional to weight, and if there are two airplanes, one small and one large, with the same payload, the smaller one is structurally more efficient, considering it requires a lighter structure to perform the same mission. Thus, airplane weight is an excellent indicator of configuration efficiency and it was considered the objective to be minimized in the mono-objective simulations. The constraints that were taken into account are: handling qualities, rudder shadowing at stall condition of the horizontal tail, and the area of solar panels, which have to be smaller than the available area on the wing.

Multi-objective simulations were run as well. In this case, weight and energy surplus were taken as objectives and an electrical demand of 200 W for the payload was considered.

DISCIPLINES

The airplane under consideration in the present study must operate at high altitudes and its loiter is performed at very low speeds, which implies a low Reynolds number relative to wing mean aerodynamic chord. Typical Reynolds number

lies in the 150,000 – 200,000 range. Due to the low speed on station, high values of lift coefficient (C_l) are experienced by the airplane wing. Taken into account that energy supply is critical, a low-drag configuration is mandatory. Based on Zephyr configuration, a typical C_l of 0.83 at 17 km of altitude was estimated, considering a speed of 60 km/h. In this condition, almost 80% of span operates at $C_l > 0.8$, as shown in Fig. 11. Thus, the biggest aerodynamic issue was to find out a low-drag airfoil for high local lift coefficients. Due to low Reynolds number, a laminar airfoil was considered, with "drag bucket" covering the desired C_l range (Fig. 12). The NACA 6-digit family

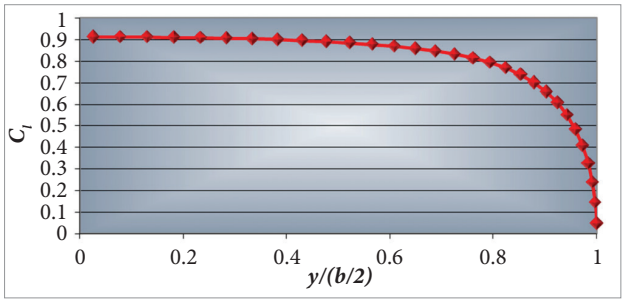

Figure 11. Lift coefficient distribution along wingspan for a Zephyr-like airplane. Calculation performed with Athena Vortex Lattice (Sion Power™, 2013).

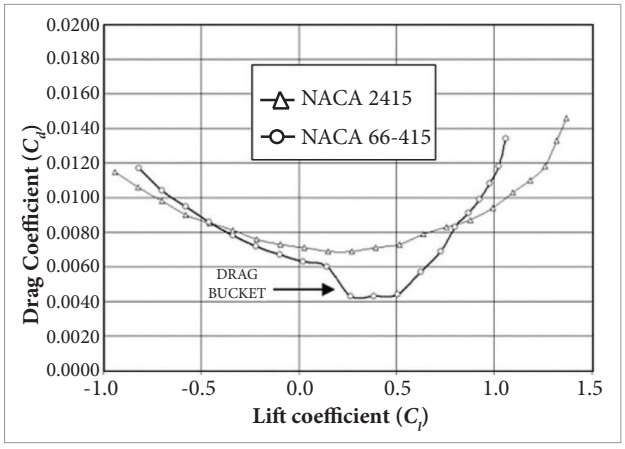

Figure 12. Typical drag polar of laminar airfoils.

offers a variety of laminar airfoils and therefore the NACA 63412 profile was selected to compose the wing. It combines all desired characteristics for the solar-powered UAV under consideration: high maximum lift coefficient (C_{lmax}); moderate to low value for the moment coefficient (C_m); and 12% relative thickness, an adequate one. All the polar curves were computed with the panel code XFOIL (Drela, 2000) and adjusted to fit to experimental results published by Abbott and Doenhoff (Abbott and Doenhoff, 1959) (Fig. 13). Table 3 contains some figures obtained with XFOIL and from experimental data. The correction for the polar curve was obtained by fitting a parabola to the non-laminar portion of the polar curve (Eq. 2):

$$C_d = C_{d,\,XFOIL} + 0.0006 \quad (2)$$

Where C_d is the drag coefficient.

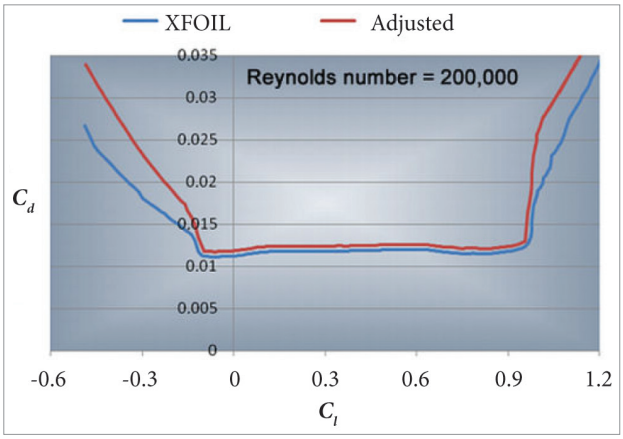

C_d: drag coefficient; C_l: lift coefficient.

Figure 13. Adjusted polar curve for NACA 63412 airfoil according to experimental data.

Table 3. Abbott and XFOIL correlation.

Source	$C_{d,laminar}$	C_{dm}	C_{lm}	k
Abbott	0.0051	0.0063	0.214	0.00732
XFOIL	0.0045	0.0061	0.177	0.00557

The NACA 63010 airfoil was chosen for the horizontal and vertical tailplanes (Fig. 14). Aerodynamic calculations for the complete configuration were performed with the incompressible Athena Vortex Lattice (AVL) vortex-lattice code (Youngren and Drela, 1988). AVL handles lifting surfaces, fuselages, and booms. All required aerodynamic and stability derivative coefficients can be quickly calculated with AVL (Youngren and Drela, 1988).

Concerning load calculation, there is no applicable certification regulation for this kind of aircraft. Estimations that were carried out for the *V-n* diagram elaboration brought no realistic results. In this effort, FAA FAR-23 and JAR-VLA

regulations were considered for a Zephyr-like airplane. For this reason, the present work considered a maximum a load factor of 3.8 for the structural sizing (Fig. 15).

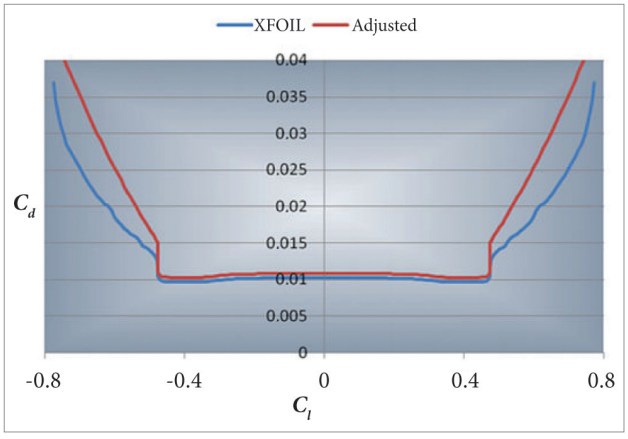

C_d: drag coefficient; C_l: lift coefficient.

Figure 14. Adjusted polar curve for NACA 63010 airfoil according to experimental data.

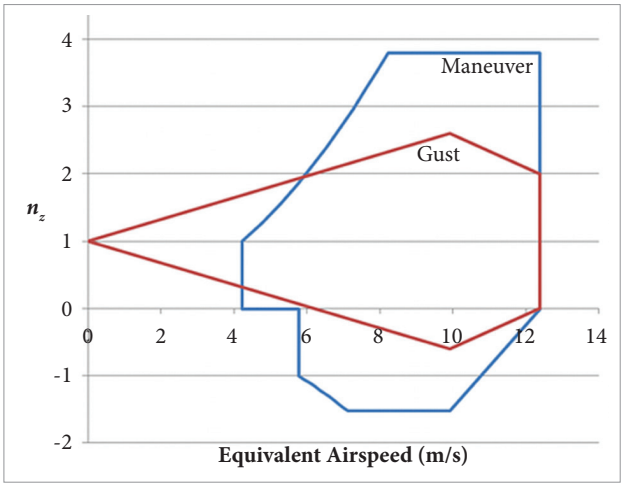

Nz: load factor.

Figure 15. Estimate *V-n* diagram for the Zephyr airplane.

The cruise speed defined by the minimum required engine power for leveled and straight flight. The upper limit of the airplane dive speed was set to be 25% above the cruise speed. The maximum load factor 3.8 was applied for wing sizing; horizontal and vertical tail stabilizers sizing considered the cruise condition, C_{Lmax}, and control surface deflection of 15º; and boom was sized considering simultaneous tails forces. Fuselage and engines were not calculated. The methods of analysis employed in the present study were very simple, as described by Megson (1999). The bending moment is supported by stringers only and torsion loads, by both stringers and skin. The structural layout is shown in Fig. 16, extending from leading edge to 25% of chord, where aerodynamic center is localized. The thickness of the wing skin is the same along the entire span, but stringers may vary for each wing station.

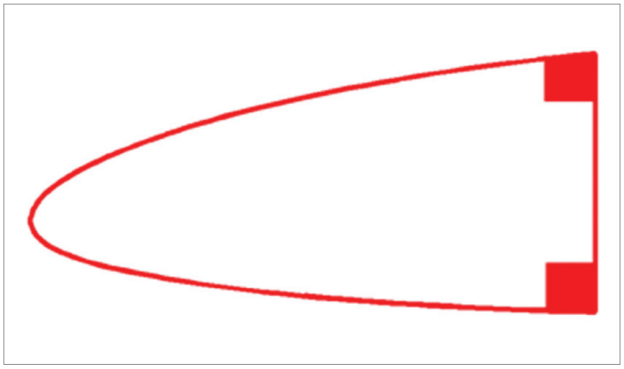

Figure 16. Wing structural layout.

Ribs were not computed but it was assumed putting three of them per meter, with constant thickness.

The boom has a cylindrical form with constant radius and thickness, approximated by thin-walled tube. It can easily withstand the existing loads for this kind of airplane. Its deflection was a constraint and used as sizing criteria. Carbon fiber was the standard material for solar airplanes, except skin, which is built of Mylar. Biaxially-oriented polyethylene terephthalate (BoPET) is a polyester film made from stretched polyethylene terephthalate (PET) and is used for its high tensile strength, chemical and dimensional stability, transparency, reflectivity, gas and aroma barrier properties, and electrical insulation. A variety of companies manufacture BoPET and other polyester films under different brand names. In the UK and the United States, the most well-known trade names are Mylar, Melinex and Hostaphan (Staugaitis and Kobren, 1996).

Densities of the selected materials for the airplane structure are well known and thus the calculation of the mass distribution is an easy task. The fuselage and payload had fixed weight; the weight of batteries depends on the capacity to supply all systems during night; and engine weight was estimated based on methodology described by Noth (2008). Thus, the weight and moment of inertia of each component can be estimated. These calculations are performed through an iterative process

until convergence is reached according to some stopping rules. Demand for electric power depends strongly on the drag, which, in turn, depends on the lift coefficient.

Stability and control is a top issue in aircraft design, particularly hard for autonomous airplanes. Unplanned situations may happen and, in this case, there is no pilot to control and stabilize the airplane. Although an on-board computer can control an unstable airplane, this paves the way for accidents. For this reason, flying qualities levels 1 or 2 were imposed, according to MIL-F8785C (Department of Defence of United States of America, 1980), adapted for UAVs (Peters and Andrisano, 1997). This leads to the implementation of lateral-directional analyses in the design framework, addressing short-period, phugoid, roll, divergent spiral and Dutch-roll characteristics.

RESULTS

The modeFrontier® workflow for the task under consideration is displayed in Fig. 17. There are ten design variables in total. They are related to the wing, horizontal tail (HT), and vertical tail (VT). The AVL panel code was employed to calculate the aerodynamic coefficients and stability derivatives. Some MATLAB® routines then evaluated the C_{Lmax} and dynamic behavior of the individuals that arise in the simulation process from data provided by AVL.

The simulations were run on a desktop computer fitted with a single Intel Core2Quad Q6600 2.40 GHz processor, and 8.0 GB of installed Random Access Memory (RAM).

The initial population was generated with the SOBOL algorithm, available in the modeFrontier® framework. SOBOL guarantees that any region of the design space does not become saturated, assuring that the entire domain be fulfilled with a great variety of individuals.

The multi-objective MOGA-II genetic algorithm (ESTECO, 2011) was chosen for running the simulations. MOGA-II is an efficient multi-objective genetic algorithm that uses a smart multi-search elitism. This new elitism operator is able to preserve some excellent solutions without bringing premature convergence to local-optimal frontiers. The efficiency of this algorithm has been orderly proved on six well known test functions for multi-objective optimization.

For simplicity, MOGA-II requires only very few user-provided parameters; several other parameters are internally settled in order to provide robustness and efficiency to the optimizer. The algorithm attempts a total number of evaluations that is equal to the number of points in the Design of Experiment (DOE) table (the initial population) multiplied by the number of generations.

MONO-OBJECTIVE SIMULATION

The first runs revealed that a large number of individuals violated the posed restrictions. It is easy to understand, because in first generations genetic algorithm searches in all

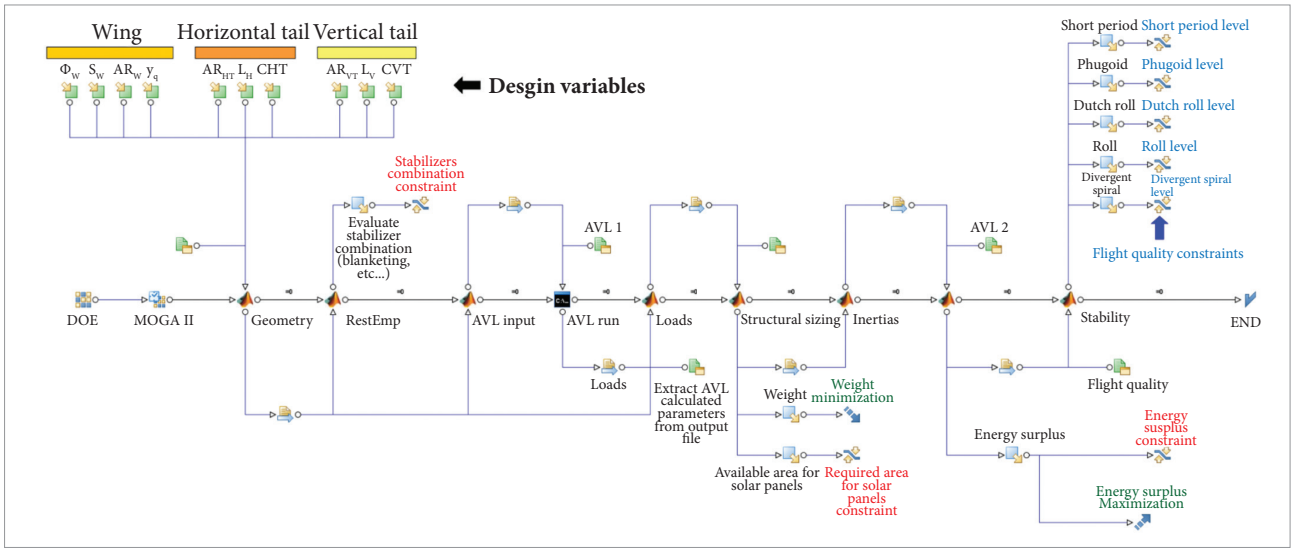

Figure 17. ModeFrontier® workflow for solar-powered unmanned aerial vehicles optimization.

considered domain and more advanced generations are next to optimum. So, algorithm naturally reduced the domain to small range that offers good individuals, except mutations.

For the simulation tasks considering payload electrical demand of 100 W, 20 generations revealed to be enough to provide satisfactory convergence for obtaining an optimal airplane configuration (Table 4). The first runs recorded a large number of individuals that violated the prescribed constraints. Along the convergence process, the optimization framework naturally narrowed the band to generate individuals and most of them fulfilled the imposed constraints (Fig. 18). In other hand, mutation may generate unfeasible individuals along the simulation process.

Table 4. Information for the standard demand simulation.

Variable	Value
Generations	20
Number of individuals	400
Repeated individuals	41
Total processing time	7h51m25s
Average processing time for a single individual	1m19s
Average processing time for four individuals	5m15s

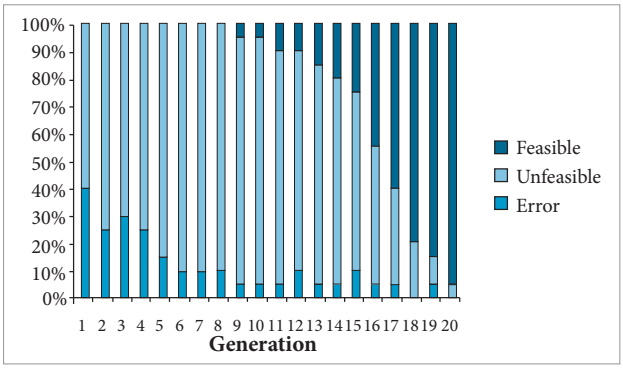

Figure 18. Feasible individual progression along the simulation process.

The violation of power supply constraint is strongly associated with small wing area, while most of other violations are related to tail configuration parameters. Figure 19 provides an overview of the constraint violation by individuals for the entire simulation.

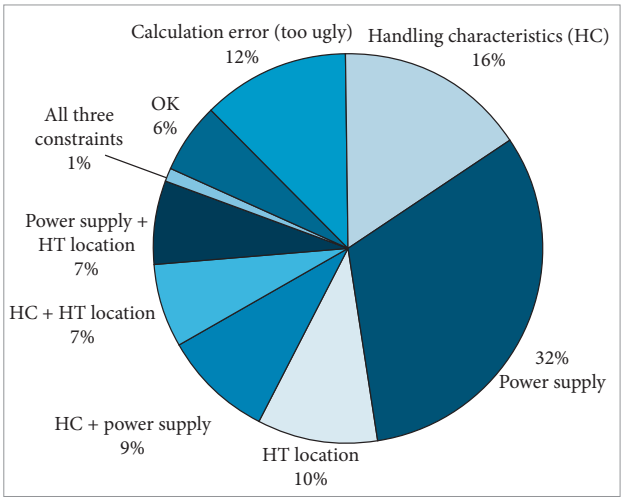

HT: horizontal tail; HC: handing characteristics.

Figure 19. Constraint violators pinpointing.

The area and weight are consistent with data from Zephyr, but its required power supply is unknown. However, the wing loading of the best individual is very close to that of Zephyr.

Considering only the best individuals that did not violate restrictions, it is possible to state that a minimum wing area of 16 m^2 is required for obtaining a feasible configuration. Larger areas can feed systems with greater capacity during the day and must be turned off at night because the battery does not have sufficient storage capacity. For example, a system that requires 350 W can work under daylight conditions and must be turned off at night for airplanes with wing area set to 20 m^2. The day chosen as the project point is very restrictive. If the same airplane flew in the summer, an 1,800 W of power could be generated during the day.

An overview of the best individual from the simulation is provided by Fig. 20. The optimal airplane presents 20 m^2 of wing area and wing aspect ratio of 25 (Table 5). All handling qualities were level 1 on station.

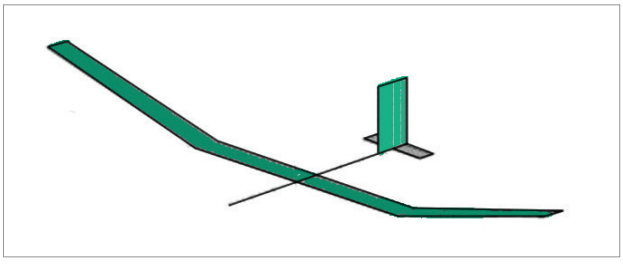

Figure 20. Optimal airplane configuration from the mono-objective simulation.

Table 5. Optimal airplane from mono-objective simulation.

S_w	20 m^2	y_q	0.40
AR_w	25	AR_{HT}	2
Outer wing dihedral angle	14°	AR_V	1.75
L_V	4.25 m	L_H	4.75 m

S_w: wing area; Y_q: break position; AR_w: wing aspect ratio; AR_{HT}: horizontal tail aspect ratio; AR_v: vertical tail aspect ratio; L_v: vertical tail lever; L_H: horizontal tail lever.

Airplane gross weight amounts 30.1 kg. The weights of the airplane components are consistent and the battery weight fraction is huge (Fig. 21), revealing that this equipment presents an issue critical for the design of a solar-powered airplane. Typically, a battery generates 350 Wh/kg (265 Wh/kg considering the wrapper), but further development can increase this figure to 600 Wh/kg, which would have great benefit for the configuration of solar-powered aircraft.

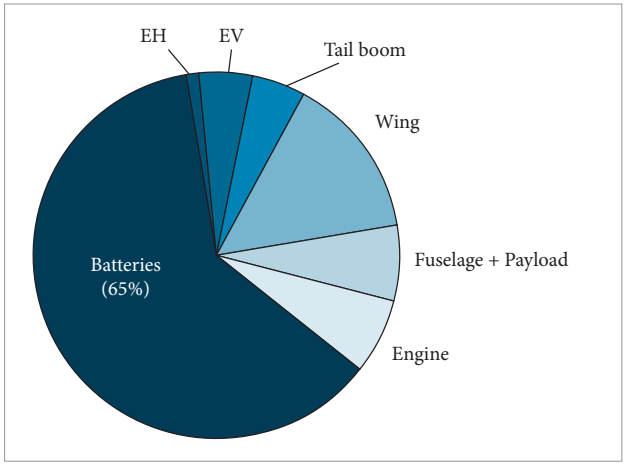

EH: horizontal tail; EV: vertical tail.

Figure 21. The above pie chart provides a weight breakdown of the optimal airplane.

As seen before, batteries are critical for design of solar powered airplanes. If the electrical power requirement for the payload is increased, the structural weight is also increased. This directly affects the weight of the engine and the required thrust to propel the airplane.

Multi-objective optimization

Weight minimization and power surplus maximization were taken as objectives for this task. Wing area was allowed to vary between 30 and 60 m^2. After 40 generations with 30 individuals each, the simulation was stopped. Figure 22 shows the feasible individuals of the present simulation and Fig. 23, its Pareto front.

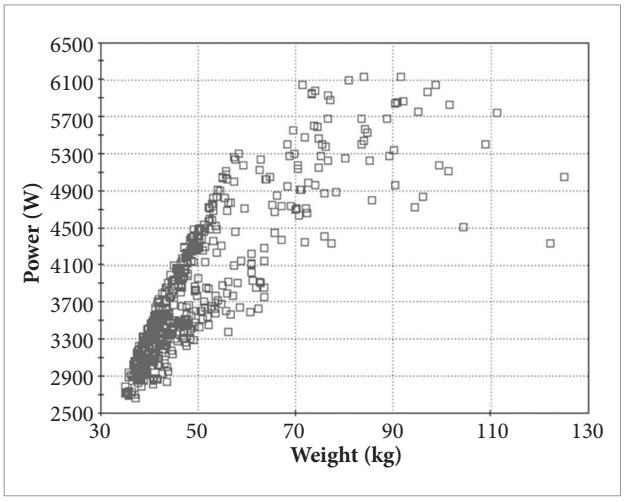

Figure 22. Feasible individuals from the multi-objective simulation.

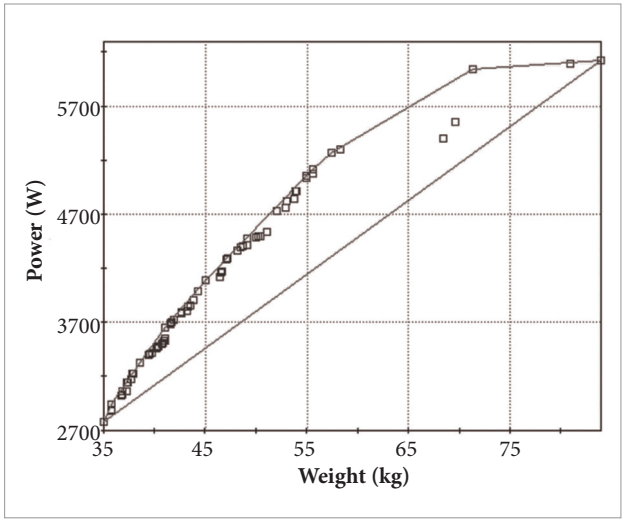

Figure 23. Pareto front of the multi-objective simulation.

Here, the available power from the optimal individuals is considerably higher than that of the optimal airplane from the previous simulation. This can be credited to the lower boundary that was set for the wing area, which was 50% higher than that of the optimal airplane from the mono-objective simulation. The configuration from the Pareto front with the lowest available power weighs just 35.21 kg, slightly over the weight of the optimal airplane from the previous simulation. Table 6 contains some characteristics of this airplane.

Table 6. Characteristics of the optimal lowest power airplane from the multi-objective simulation.

S_w	30 m^2	y_q	0.55
AR_w	21	AR_{HT}	3.25
Outer wing dihedral angle	12°	AR_V	1.50
L_V	4.75 m	L_H	6.50 m

S_w: wing area; Y_q: break position; AR_w: wing aspect ratio; AR_{HT}: horizontal tail aspect ratio; AR_V: vertical Tail aspect ratio; L_V: vertical tail lever; L_H: horizontal tail lever.

CONCLUDING REMARKS

The development of solar-powered airplanes in the past was directly affected by the technology of solar panels. Nowadays, alongside with the solar panel efficiency issue, energy storage became a major concern for the design of solar air vehicles. In addition, considering that there are few airplanes flying in altitudes from 15 to 18 km, there are also few aircraft systems manufacturers able to deliver products capable of working under severe environmental conditions like the ones found in such altitudes.

The application of optimization tools proved to be quite appropriate, as provided in less than one day running a very large variety of airplanes, for which one can identify the strengths, weaknesses, and typical values of the variables for a good design. The case study proposed is an excellent example of this, because there are few semi-empirical mathematical models and built aircraft data, and even then with the application of simple theories, it was possible to design and verify the consistency with the few existing models.

Future work will encompass the wing and tail airfoils as design variables.

ACKNOWLEDGMENTS

The authors thank Fundação de Amparo à Pesquisa do Estado de São Paulo (FAPESP) for its support by the project 2007/00305-5.

REFERENCES

Abbott, I.H. and Doenhoff, A.E., 1959, "Theory of wing sections", Dover Publications, Mineola, NY, USA. 693 p.

Anderson, J.D., 1989, "Introduction to Flight," 3rd Edition, McGraw-Hill, USA.

Department of Defence of United States of America, 1980, "MIL-F-8785C: Military Specification Flying Qualities of Piloted Airplanes", Washington, DC.

Drela, M., 2000, "X-FOIL subsonic development system" [Internet], Massachusetts Institute of Technology (MIT).Available from: http://web.mit.edu/drela/Public/web/xfoil/. Accessed: June, 2006.

ESTECO s.p.a., modeFrontier® 4 User Manual, 2011.

Flisom – Flexible Solar Modules [Internet]. Available from: http://www.flisom.ch. Accessed: April 26, 2013.

Joint Research Centre, Institute for Energy and Transport (IET), "Solar Radiation and GIS" [Internet]. Available from: http://re.jrc.ec.europa.eu/pvgis/solres/solmod3.htm. Accessed: April 26, 2013.

MacCready, P.B., Lissaman, P.B.S., Morgan, W.R., and Burke. J.D., 1983, "Sun-Powered Aircraft Designs", Journal of Aircraft, Vol. 20, No 6, pp. 487-493.

Megson, T.H.G., 1999, "Aircraft structures for engineering students", 3rd Edition, Butterworth Scientific, Oxford.

Noth, A., 2008, "Design of Solar Powered Airplanes for Continuous Flight," Ph.D. Thesis, École Polytechnique Fédérale de Lausanne, Swiss.

Peters, M.E. and Andrisano, D., 1997, "The determination of longitudinal flying qualities requirements for light weight unmanned aircraft," AIAA Guidance, Navigation, and Control Conference, New Orleans, LA, Aug. 11-13.

QinetiQ [Internet]. Available from: http://www.qinetiq.com/. Accessed: April 26, 2013.

Romeo, G. and Frulla, G., 2004, "Heliplat: High Altitude Very-Long Endurance Solar Powered UAV for Telecommunication and Earth Observation Applications", The Aeronautical Journal, Vol. 108, pp. 277-293.

Roskam, J., 2000, "Airplane Design, Part VI: Preliminary Calculation of Aerodynamics, Thrust and Power Characteristics", The University of Kansas, Lawrence. DARcorporation.

Sion Power™ [Internet]. Available from: http://www.sionpower.com/. Accessed: April 26, 2013.

Solar Impulse [Internet]. Available from: http://www.solarimpulse.com/. Accessed; April 26, 2013.

Staugaitis, C. and Kobren, L., 1996, "Mechanical and Physical Properties of the Echo II Metal-Polymer Laminate," NASA TN D-3409, NASA Goddard Space Flight Center.

Volz Servos [Internet]. Available from: http://www.volz-servos.com/en/index.php?m=m. Accessed: April 26, 2013.

Youngren, H. and Drela, M., 1988, "Athena vortex lattice (AVL): an extended vortex-lattice model for aerodynamic analysis, trim calculation, dynamic stability analysis, and aircraft configuration development" [Internet]. Available from: http://web.mit.edu/drela/Public/web/avl/. Accessed: February, 2007.